Effects of a fixation screw on trabecular structural changes in a vertebral body predicted by remodeling simulation

Tsubota, Ken-ichi
Adachi, Taiji
Tomita, Yoshihiro

(Citation)
Journal Annals of Biomedical Engineering,31(6):733-740

(Issue Date)
2003-06

(Resource Type)
journal article

(Version)
Accepted Manuscript

(URL)
https://hdl.handle.net/20.500.14094/90000019

Effects of a Fixation Screw on Trabecular Structural Changes in a Vertebral Body Predicted by Remodeling Simulation

Ken-ichi Tsubota,* Taiji Adachi,†* and Yoshihiro Tomita†*

* Computer and Information Division, Advanced Computing Center
The Institute of Physical and Chemical Research (RIKEN)
2-1 Hirosawa, Wako, Saitama 351-0198, Japan

† Department of Mechanical Engineering, Faculty of Engineering
Kobe University
Nada, Kobe 657-8501, Japan

Corresponding author:	Ken-ichi Tsubota, Ph.D.
Mailing address:	Computer and Information Division, Advanced Computing Center
	The Institute of Physical and Chemical Research (RIKEN)
	2-1 Hirosawa, Wako, Saitama 351-0198, Japan
Telephone:	+81(48) 467-4536
Fax:	+81(48) 467-8705
E-mail:	tsubota@postman.riken.go.jp

Abstract

Computational simulation of trabecular surface remodeling was conducted to investigate the effects of a spinal fixation screw on trabecular structural changes in a vertebral body. By using voxel-based finite elements, computational models of the bone and screw were constructed in two structural scales of a vertebral body with an implanted screw and a bone-screw interface. In the vertebral body, the implantation of the fixation screw caused changes in the mechanical environment in cancellous bone, leading to trabecular structural changes at the cancellous level. The effects of the screw on trabecular orientation were greater in the regions above and below the screw than in those in front of the screw. In the case of the bone-screw interface, trabecular structural changes depended on the direction of load applied to the screw. It was suggested that the bone resorption predicted in the pull-out loading case is a candidate cause of the loosening of the screw. The results indicate that the effects of the implanted screw on trabecular structural changes are more important for longer-term fixation.

Key Terms

Computational biomechanics, Bone structural adaptation, Trabecular surface remodeling, Spinal fixation, Bone implant, Voxel-based finite element model, Large-scale computation

1. INTRODUCTION

[#S2-1] In spinal fixation with a screw, the biomechanical viewpoint is important in order to avoid loosening of a fixation screw and to attain mechanical stability of the reconstructed spinal structure [17, 29]. As a cause of screw loosening, fatigue fracture of the bone at the bone-screw interface has been investigated using a quantitative experimental technique [15]. On the other hand, bone structural changes due to mechanical remodeling are suggested to play an important role in the loosening phenomenon [7, 15]. However, few studies have focused on mechanical bone remodeling in a vertebral body with a fixation screw.

To predict and evaluate the bone remodeling phenomenon, computational simulation methods have been used as powerful tools in the orthopaedic field [13, 21]. To date, remodeling simulations based on the macroscopic continuum model have predicted changes in apparent bone density around the hip joint stem [8, 12, 22] and knee prosthesis [19]. Furthermore, surface remodeling simulations have been applied to trabecular microstructural changes at screw threads and on porous coated surfaces of bone implants [16, 25]. These computational methods are also applicable to the design of bone implants with the desired shape where the bone structural change by remodeling is taken into consideration [14].

For the mechanical bone remodeling in spinal fixation, cancellous bone is more important than cortical bone because fixation screws are implanted mostly into the cancellous bone of the vertebral body. Remodeling in cancellous bone occurs on trabecular surfaces [20] due to cellular activities regulated by a local mechanical stimulus [6], leading to the structural change of each trabecula. Microstructural changes of the trabeculae result in changes of the macrostructure of cancellous bone, such as apparent bone density and orientation. To express these hierarchical structural changes from the single-trabecular level up to the cancellous level, voxel-based finite element models with a large-scale computational technique are useful for the simulation of trabecular surface remodeling [2].

The purpose of this study is to investigate the effects of a fixation screw on three-dimensional trabecular structural change in a vertebral body, using voxel-based finite element models of trabecular surface remodeling. First, a remodeling simulation is conducted for a vertebral body to examine the effects of the implanted screw on structural changes at the cancellous level. Second, trabecular microstructural changes adjacent to the bone-screw interface are simulated to investigate the relationships between the loosening of the screw and the loads applied to the screw. Third, referring to the simulation results, important mechanical factors in the implantation of the screw are discussed from the viewpoint of mechanical bone remodeling.

2. METHODS

2.1. Model of a Vertebral Body with a Fixation Screw (Model S)

A spinal fixation screw, such as that used in internal fixation for fusion [17,29] and in total *en bloc* spondylectomy for a vertebral tumor [27], plays an important role in maintaining the mechanical integrity of the reconstructed spinal structure. In this study, a half-model of a human L3 vertebral body with a fixation screw (model S) was created using about 0.79 million voxel-based finite elements, as shown in Fig. 1, assuming symmetry with respect to the center sagittal plane. The model consisted of cortical bone, cancellous bone, and a fixation screw, in which the cortical and cancellous parts were taken from a model of the normal vertebral body (model N) shown in the Appendix. [#G-1] Morphologies of each trabeculae were directly expressed as shown in Fig. 1, instead of using apparent material properties of cancellous bone. The size of the vertebral body was 50 mm in diameter in the bilateral and anteroposterior directions, and 25 mm in height in the axial direction, as shown in Fig. 1(a). The X_1 axis was set to correspond to the bilateral direction, the X_2 axis to the anteroposterior direction, and the X_3 axis to the axial direction. [#S2-2] The trabecular structure at the initial stage was taken from a result of trabecular remodeling simulation with model N shown in the Appendix. The trabeculae aligned along the axial direction according to the compressive load of body weight, as shown in $X_2 - X_3$ and $X_1 - X_3$ cross sections in Fig. 1(b). The screw was set to be $4\ \mathrm{mm}$ in diameter and $50\ \mathrm{mm}$ in length of which $24\ \mathrm{mm}$ was implanted into the vertebral body. The size of each element was $250\ \mu\mathrm{m}$.

As a boundary condition of the vertebral body under the compressive load of body weight, uniform compressive displacement U_3 was applied to the upper plane at $X_3 = 25\ \mathrm{mm}$ to apply the total load $F_1 = 588\ \mathrm{N}$, as shown in Fig. 1(a). The lower plane at $X_3 = 0\ \mathrm{mm}$ was fixed. In applying compressive load to the vertebral body, the displacement constraint U_3 is equivalent to the force constraint F_1, which is advantageous for saving computational time in the large-scale finite element method [11, 23]. As the load transferred from the fixation device, the bending load $F_2 = 58.8\ \mathrm{N}$ was applied to the end of the screw. The bone and screw were assumed to be homogeneous and isotropic materials, and Young's modulus E and Poisson's ratio ν were set as $E_b = 20\ \mathrm{GPa}$ and $\nu_b = 0.3$ for the bone, and $E_s = 200\ \mathrm{GPa}$ and $\nu_s = 0.29$ for the screw which was assumed to be stainless steel [3, 31]. The marrow was considered as a cavity, and neglected in the finite element analysis [2,16,25].

2.2. Model of Bone-Screw Interface (Model I)

The trabecular structure adjacent to the bone-screw interface is important for proper fixation of a screw to cancellous bone [19]. As a model of the bone-screw interface, a $7 \times 7 \times 14\ \mathrm{mm}^3$ cancellous bone hexahedron was created (model I) using about 0.91 million voxel-based finite elements, as shown in Fig. 2(a), in which the size of each voxel was $70\ \mu\mathrm{m}$. The cancellous bone part of model I was filled with ring-shaped trabeculae assuming that the initial trabecular structure was isotropic. The external and root diameters of the screw were $4.9\ \mathrm{mm}$ and $3\ \mathrm{mm}$, respectively, and the pitch was $1.8\ \mathrm{mm}$. The coordinate axes were set as shown in Fig. 2(a), in which the X_2 axis corresponded to the screw axis.

Assuming the screw was subjected to body weight and pull-out load, two cases of simple loading, namely, compressive loading (Ic) and shear loading (Is) were considered in the remodeling simulation, as shown in Fig. 2(b). As a boundary condition, uniform compressive displacement along the X_3 axis was applied to the upper surface of the screw in case Ic, and uniform shear displacement along the X_2 axis was applied in case Is, as shown in Fig. 2(b). The displacements were controlled to apply an apparent stress of $1\ \mathrm{MPa}$ on the upper plane of the screw. The displacement constraint was advantageous for saving computational time in the finite element analysis. On the bottom and side planes of cancellous bone, shear-free boundary conditions were applied, that is, the displacements perpendicular to the plane were fixed. Simulation results were discussed only for the internal region of the finite element model, as shown by the white box in Fig. 2(a), to neglect an artificial influence of the boundary condition.

2.3. Voxel Simulation Method of Trabecular Surface Remodeling

For models S and I, trabecular structural changes were simulated based on a rate equation of trabecular surface remodeling in which the remodeling was assumed to be driven by local nonuniformity of equivalent stress [1]. The model parameters in the remodeling model [28] were set constant as threshold values $\Gamma_u = 1.0$ and $\Gamma_l = -1.25$, and sensing distance $l_L = 2.5$ mm for model S, and $\Gamma_u = 1.5$, $\Gamma_l = -1.88$, and $l_L = 700$ μm for model I. The trabecular morphological changes due to remodeling were accomplished by repetitive cycles of a large-scale finite element analysis and removal/addition of the voxel elements from/to the trabecular surface [2]. For the condition of the bone-screw interface in stress analysis, it was assumed that tensile load perpendicular to the interface was not transferred from the screw to the bone.

In the following section, the simulation result was evaluated for regions F (in front of the screw tip), A (above the screw), and B (below the screw) for model S, and regions C (below the screw), S_1 (on the negative side on the X_1 axis), and S_2 (on the positive side) for model I. In these regions, fabric ellipsoid [5] was measured as an anisotropic structural parameter. The degree of structural anisotropy was defined as the ratio of the maximum principal value of the fabric ellipsoid H_1 to the minimum value H_3, and the trabecular orientation angle θ_i $(i = 1,2,3)$ was defined as the angle between the maximum principal direction of the fabric ellipsoid $\boldsymbol{n}^{H_1}$ and the coordinate axis X_i. For model I, the contact area between the bone and the screw threads S, normalized by the initial contact area S_0, was measured to investigate the structural changes of trabeculae adjacent to the screw threads.

3. RESULTS

3.1. Structural Changes at Cancellous Level due to Implantation of the Screw

In the case of a vertebral body with a fixation screw (model S), the trabeculae adapted their structure to the mechanical environment that was changed by the implanted screw, as shown in Fig. 3. The load applied to the end of the screw caused more trabecular structural changes in regions A and B than in region F where the effect of the screw on the mechanical environment was smaller.

In region F, trabeculae grew thick in the axial direction and were resorbed in the transverse direction due to the compressive load of body weight, as shown in the $X_2 – X_3$ cross section in Fig. 3(a). The degree of structural anisotropy H_1 / H_3 and trabecular orientation angle θ_i $(i = 1,2,3)$ were $H_1/H_3 = 1.89$ and $(\theta_1,\theta_2,\theta_3) = (89^\circ, 88^\circ, 2^\circ)$, respectively. The structural parameters and fabric ellipsoid shown in Fig. 3(b) indicated that the trabeculae in region F are oriented along the axial direction.

The degree of structural anisotropy H_1/H_3 and trabecular orientation angle θ_i were, respectively, $H_1/H_3 = 1.46$ and $(\theta_1,\theta_2,\theta_3) = (90^\circ, 83^\circ, 7^\circ)$ in region A, and $H_1/H_3 = 1.41$ and $(\theta_1,\theta_2,\theta_3) = (87^\circ, 79^\circ, 11^\circ)$ in region B. In these two regions, the structural parameter H_1/H_3 was smaller and θ_3 was larger than those in region F. The result showed that the trabecular structure was more distributed in regions A and B than in region F. For example, the trabeculae in region B were formed both from the screw tip and from the pedicle to the lower cortical shell, as indicated by open arrows in the $X_2 - X_3$ cross section in Fig. 3(a). Part of these trabeculae connected with each other and formed an arcuate structure, as indicated by a closed arrow in the $X_2 - X_3$ cross section in Fig. 3(a).

3.2. Structural Changes of Trabeculae adjacent to Bone-Screw Interface

In the case of the bone-screw interface (model I), the isotropic trabecular structure shown in Fig. 2(a) changed to the anisotropic one shown in Figs. 4 and 5. As a result of remodeling driven by the stress nonuniformity on the trabecular surface, the obtained trabecular structure depended on the loads applied to the screw.

In the case of compressive loading (Ic), the trabeculae were aligned along the direction of compressive load below the screw, as indicated by arrows in the $X_2 - X_3$ cross section in Fig. 4(a), and formed radially from the screw, as indicated by arrows in the $X_1 - X_3$ cross section. The degree of structural anisotropy H_1 / H_3 and trabecular orientation angle θ_i $(i = 1,2,3)$ were $H_1 / H_3 = 1.24$ and $(\theta_1, \theta_2, \theta_3) = (86^\circ, 90^\circ, 4^\circ)$ in region C, $H_1 / H_3 = 1.23$ and $(\theta_1, \theta_2, \theta_3) = (54^\circ, 90^\circ, 36^\circ)$ in region S_1, and $H_1 / H_3 = 1.22$ and $(\theta_1, \theta_2, \theta_3) = (65^\circ, 88^\circ, 25^\circ)$ in region S_2, as shown in Fig. 4(b). The result showed that the structural orientation was different in each region with a similar degree of structural anisotropy.

In the case of shear loading (Is), some of the trabeculae below the screw were aligned along the directions oriented 45 degrees according to shear load, as indicated by arrows in the $X_2 - X_3$ cross section in Fig. 5(a). The degree of structural anisotropy H_1 / H_3 and trabecular orientation angle θ_i were, respectively, $H_1 / H_3 = 1.17$ and $(\theta_1, \theta_2, \theta_3) = (85^\circ, 12^\circ, 79^\circ)$ in region C, $H_1 / H_3 = 1.12$ and $(\theta_1, \theta_2, \theta_3) = (52^\circ, 88^\circ, 38^\circ)$ in region S_1, and $H_1 / H_3 = 1.15$ and $(\theta_1, \theta_2, \theta_3) = (78^\circ, 12^\circ, 90^\circ)$ in region S_2, as shown in Fig. 5(b). The finding that H_1 / H_3 values in this case are smaller than those in the case Ic indicated a more distributed trabecular structure, as shown in the $X_1 - X_3$ cross section in Fig.

5(a).

#S2-5 Change in the contact area S/S_0 depended on the site of the screw threads, as shown in Fig. 6. In case Ic, the contact area S/S_0 increased after the initial decrease at the top of the screw threads (Tt), and decreased on both sides (Ts_1 and Ts_2) and at the root (Tr), as shown in Fig. 6(a). In case Is, the entire contact area S/S_0 decreased, as shown in Fig. 6(b). The rates of decrease of the contact area S/S_0 at the root (Tr) and on the tensile side (Ts_1) were higher than those at the top (Tt) and on the compressive side (Ts_2), and the area S/S_0 at Tr and Ts_1 became zero at the final state.

4. DISCUSSION

It has been suggested that trabecular structural changes due to mechanical bone remodeling are important for the proper fixation of a bone implant, such as a hip joint stem in the proximal femur [8, 12, 22] and a dental implant in the mandible [26]. However, it has not been reported whether the trabecular structure changes when a fixation screw is implanted into a vertebral body. This is due to the difficulty in both observing *in vivo* trabecular structural changes around the fixation screw and simulating the trabecular structural changes around the screw, by previous computational techniques. In this study, the trabecular structural changes around the screw were simulated using voxel-based finite element models of trabecular surface remodeling. As a result of using model S for a vertebral body with a fixation screw, it was predicted that trabecular orientation in the pedicle region changed due to changes in the mechanical environment caused by the implanted screw. Because the change in trabecular orientation affects the mechanical integrity of the vertebral body, the simulation method will be useful in evaluating time-course changes, due to trabecular bone remodeling, in the mechanical integrity of a vertebral body with a screw.

Model S was constructed to investigate the basic effects of the screw on the trabecular structural changes in the vertebral body. For accurate prediction of the trabecular structural changes in the future, it is necessary to develop a model of the ligamentous motion segment in which intervertebral discs play an important role in transferring the body weight to the vertebral body. For example, if a model of intervertebral discs that consist of annulus fibrousus and nucleus pulposus is developed to express precise loading conditions of the vertebral body, the predicted trabeculae using model N for a normal vertebral model (see Appendix) would be less in the pedicle part than in the central part, as was predicted by Goel *et al*. [9]. This might cause the denser trabeculae to occur at the center of the vertebral body when the fixation screw is implanted, because the load applied to the screw will be supported less by the trabeculae in the pedicle region and more by those in the central region.

In a remodeling simulation using model I for the bone-screw interface, the trabecular structural changes corresponded to the loads applied to the screw, as shown in Figs. 4 and 5. While the trabeculae remained near the screw threads with compressive load (case Ic), the bone was resorbed on the tensile side (Ts_1) and at the root (Tr) of the threads with shear load (case Is). These results show that the direction of load applied to the screw is one of the critical factors in determining bone resorption at the bone-screw interface, and that pull-out loading is a candidate cause of screw loosening. The bone resorption predicted by the simulation depended on the site of the screw threads, which indicates that the screw threads are important in the loosening of the fixation screw due to remodeling. In fact, the remodeling simulation using model S did not predict the trabecular structural changes that would cause the loosening of the screw because the screw threads were not modeled in detail. In addition, progress of the structural changes in time, as shown in Fig. 6, demonstrates that remodeling around the spinal fixation screw is more important for longer-term fixation.

For model I, the isotropic initial trabecular structure was used instead of an anisotropic one as was used in model S. The loading conditions applied to the screw were assumed to be two cases of simple loading, namely, compressive and shear loading. Despite these simplifications, the bone resorption around the screw thread obtained in case Is indicates that the stress-shielding phenomenon can exist in a vertebral body with a fixation screw, as well as in the case of other bone implants [22, 26]. The effects of structural anisotropy and complicated loading conditions in the actual bone will be taken into account by coupling the two-structural scales of models S and I in future work.

Based on experimental and computational studies on trabecular structural changes around implants [2, 10, 22], the structural changes obtained in this study can be regarded to occur within from a few months to a few years. With this time scale, it would be necessary, in spinal fixation, to consider the trabecular remodeling phenomenon to evaluate the vertebral body with the fixation screw as a load-bearing structure. For example, an experimental result obtained using canine spine surgery model, in which the spine from L1 to L5 was immobilized for nine months using an instrument with transpedicular screws placed bilaterally at the L1, L3 and L5 pedicles, indicated that loosening of the screw was observed more for L1 and L5 than for L3 [7]. [#S2-6] In the immobilized spinal structure, the screws at L1 and L5 outside of the instrument are subjected to bending load transferred from the fixation device more than those placed at L3 in the middle of the instrument. Because the bending load of the screw would cause pull-out load of the screw, the screw loosening at the L1 and L5 obtained in the animal experiment might be due to the pull-out load applied to the screw. This point corresponds to the simulation result of model I for the bone-screw interface, which indicates the pull-out load is a candidate cause of the screw loosening.

The simulation method using a voxel model is effective in predicting remodeling phenomena in individual cases because the voxel model of bone structure can be easily constructed from medical image data [24]. Thus, the voxel-based simulation method will enable us to test various combinations of bone and spinal fixation screws, and will provide us with useful information for choosing the screw type. In addition, considering that voxel models of a musculoskeletal system, including that of a spinal system, can be constructed using recent imaging techniques [4, 30], voxel models of a bone-implant system for various types of implants can be constructed by superimposition of the digital implant data (that is, CAD data) to the spinal voxel model. With this voxel model, the remodeling simulation method will be useful for designing a spinal fixation system for individuals. The combination of the bone remodeling simulation using the voxel model with advanced techniques for medical imaging and structural optimization will provide a new computational design system for bone-implant devices.

ACKNOWLEDGMENTS

The support of the Special Postdoctoral Researchers Program through The Institute of Physical and Chemical Research (RIKEN) is gratefully acknowledged. This work was supported financially in part by a Grant-in-Aid for Scientific Research from the Ministry of Education, Culture, Sports, Science and Technology of Japan.

APPENDIX. Trabecular Structural Change for Normal Vertebral Body (Model N)

In the case of a normal vertebral body, trabecular surface remodeling simulation was conducted using a half-voxel model of a human L3 vertebral body (model N), as shown in Fig. 7(a). The cortical shape of the model in the midsagittal plane was determined based on a photograph of the cross section of the human vertebral body available in the literature [18], as shown in Fig. 7(b). Rotating the midsagittal section with regard to the center longitudinal axis, the three-dimensional shape of the cortical bone was constructed as an axisymmetric shell. The size of the vertebral body was $50\ \mathrm{mm}$ in diameter in the bilateral and anteroposterior directions, and $25\ \mathrm{mm}$ in height in the axial direction.

The cancellous bone part was filled with ring-shaped trabeculae to a bone volume fraction of $BV/TV = 0.46$ and the degree of structural anisotropy of $\square_1/\square_3 = 1.04$, in which $\square_1$ and $\square_3$ were the maximum and minimum principal values of fabric ellipsoid [5], respectively. As indicated by fabric ellipsoid and $X_2 \square X_3$ cross section in Fig. 7(a), the trabecular structure was isotropic at the initial state. The number of voxel elements of bone was about 0.85 million, and the size of each element was $250\ \mu\mathrm{m}$. The bone part was assumed to be homogeneous and isotropic materials, and Young's modulus E and Poisson's ratio ν were set as $E_b = 20\ \mathrm{GPa}$ and $\nu_b = 0.3$ [3,31]. The marrow was considered to be a cavity, and neglected in the finite element analysis. As a boundary condition, uniform compressive displacement U_3 was applied to the upper plane at $X_3 = 25\ \mathrm{mm}$ to apply the total load $F_1 = 588\ \mathrm{N}$ as a body weight. The lower plane at $X_3 = 0\ \mathrm{mm}$ was fixed. The model parameters in the remodeling rate equation [28] were set constant as threshold values $\Gamma_u = 1.0$ and $\Gamma_l = -1.25$, and sensing distance $l_L = 2.5\ \mathrm{mm}$.

As a result of the remodeling simulation, an anisotropic trabecular structure was obtained due to trabecular formation and resorption driven by local stress nonuniformity, as indicated by the $X_2 - X_3$ cross section and fabric ellipsoid of the trabecular structure in Fig. 8. The angle θ_3 between the maximum principal direction of the fabric ellipsoid and the X_3 axis was 3°, which was consistent with the observed phenomenon that the trabeculae in the vertebral body are oriented along the axial direction [18]. Bone volume fraction BV/TV decreased to 0.37, and the degree of structural anisotropy H_1/H_3 increased to 1.47. The structural parameters BV/TV and H_1/H_3 obtained in the simulation better expressed the experimental observation [4] than those of the initial isotropic structure.

REFERENCES

1. Adachi, T., Y. Tomita, H. Sakaue, and M. Tanaka. Simulation of trabecular surface remodeling based on local stress nonuniformity. *JSME Int. J.* 40C-4: 782-792, 1997.

2. Adachi, T., K. Tsubota, Y. Tomita, and S. J. Hollister. Trabecular surface remodeling simulation for cancellous bone using microstructural voxel finite element models. *Trans. ASME, J. Biomech. Eng.* 123-5: 403-409, 2001.

3. An, Y. H. "Mechanical properties of bone". In: *Mechanical testing of bone and the bone-implant interface*, edited by Y. H. An, and R. A. Draughn. CRC Press, 1999, pp. 41-63.

4. Beuf, O., D. C. Newitt, L. Mosekilde, and S. Majumdar. Trabecular structure assessment in lumbar vertebrae specimens using quantitative magnetic resonance imaging and relationship with mechanical competence. *J. Bone Miner. Res.* 16-8: 1511-1519, 2001.

5. Cowin, S. C. The relationship between the elasticity tensor and the fabric tensor. *Mechanics of Materials* 4: 137-147, 1985.

6. Cowin, S. C., L. Moss-Salentijn, and M. L. Moss. Candidates for the mechanosensory system in bone. *Trans. ASME, J. Biomech. Eng.* 113-2: 191-197, 1991.

7. Dalenberg, D. D., M. A. Asher, R. G. Robinson, and G. Jayaraman. The effect of a stiff spinal implant and its loosening on bone mineral content in canines. *Spine* 18-13: 1862-1866, 1993.

8. Doblaré, M., and J. M. García. Application of an anisotropic bone-remodelling model based on a damage-repair theory to the analysis of the proximal femur before and after total hip replacement. *J. Biomech*. 34-9: 1157-1170, 2001.

9. Goel, V. K., S.A. Ramirez, W. Kong, and L.G. Gilbertson. Cancellous bone Young's modulus variation within the vertebral body of a ligamentous lumbar spine - application of bone adaptive remodeling concepts. *Trans. ASME, J. Biomech. Eng*. 117-3: 266-271, 1995.

10. Guldberg, R. E., M. Richards, N. J. Caldwell, C. L. Kuelske, and S. A. Goldstein. Trabecular bone adaptation to variations in porous-coated implant topology. *J. Biomech*. 30-2: 147-153, 1997.

11. Hughes, T. J. R., R. M. Ferencz, and J. O. Hallquist. Large-scale vectorized implicit calculations in solid mechanics on a Cray X-MP/48 utilizing EBE preconditioned conjugate gradients. *Comp. Meth. Appl. Mech. Eng*. 61: 215-248, 1987.

12. Huiskes, R., H. Weinans, H. J. Grootenboer, M. Dalstra, B. Fudala, and T. J. Slooff.

Adaptive bone-remodeling theory applied to prosthetic-design analysis. *J. Biomech.* 20-11/12: 1135-1150, 1987.

13. Huiskes, R., and S. J. Hollister. From structure to process, from organ to cell: recent developments of FE-analysis in orthopaedic biomechanics. *Trans. ASME, J. Biomech. Eng.* 115-4(B): 520-527, 1993.
14. Kuiper, J. H., and R. Huiskes. Mathematical optimization of elastic properties: application to cementless hip stem design. *Trans. ASME, J. Biomech. Eng.* 119-2: 166-174, 1997.
15. Lu, W. W., Q. Zhu, A. D. Holmes, K. D. Luk, S. Zhong, and J. C. Leong. Loosening of sacral screw fixation under in vitro fatigue loading. *J. Orthop. Res.* 18-5: 808-814, 2000.
16. Luo, G., A. M. Sadegh, H. Alexander, W. Jaffe, D. Scott, and S. C. Cowin. The effect of surface roughness on the stress adaptation of trabecular architecture around a cylindrical implant. *J. Biomech.* 32-3: 275-284, 1999.
17. McCullen, G. M., and S. R. Garfin. Cervical spine internal fixation using screw and screw-plate constructs. *Spine* 25-5: 643-652, 2000.
18. Mosekilde, L. "Age-related loss of vertebral trabecular bone mass and structure —

biomechanical consequences". In: *Biomechanics of Diarthrodial Joints II,* edited by V. C. Mow, A. Ratcliffe, and S. L-Y. Woo. Springer, 1990, pp. 83-96.

19. Orr, T. E., G. S. Beaupré, D. R. Carter, and D. J. Schurman. Computer predictions of bone remodeling around porous-coated implants. *J. Arthroplasty* 5-3: 191-200, 1990.

20. Parfitt, A. M. Osteonal and hemi-osteonal remodeling: the spatial and temporal framework for signal traffic in adult human bone. *J. Cell. Biochem.* 55: 273-286, 1994.

21. Prendergast, P. J. Finite element models in tissue mechanics and orthopaedic implant design. *Clin. Biomech.* 12-6: 343-366, 1997.

22. van Rietbergen, B., R. Huiskes, H. Weinans, D. R. Sumner, T. M. Turner, and J. O. Galante. The mechanism of bone remodeling and resorption around press-fitted THA stems. *J. Biomech.* 26-4/5: 369-382, 1993.

23. van Rietbergen, B., H. Weinans, R. Huiskes, and A. Odgaard. A new method to determine trabecular bone elastic properties and loading using micromechanical finite-element models. *J. Biomech.* 28-1: 69-81, 1995.

24. van Rietbergen, B., S. Majumdar, W. Pistoia, D. C. Newitt, M. Kothari, A. Laib, and P. Rüegsegger. Assessment of cancellous bone mechanical properties from micro-FE models based on micro-CT, pQCT and MR images. *Technol. Health Care* 6-5/6: 413-

420, 1998.

25. Sadegh, A. M., G. M. Luo, and S. C. Cowin. Bone ingrowth: an application of the boundary element method to bone remodeling at the implant interface. *J. Biomech.* 26-2: 167-182, 1993.

26. Stanford, C. M., and R. A. Brand. Toward an understanding of implant occlusion and strain adaptive bone modeling and remodeling. *J. Prosthet. Dent.* 81-5: 553-561, 1999.

27. Tomita, K., N. Kawahara, H. Baba, H. Tsuchiya, T. Fujita, and Y. Toribatake. Total en bloc spondylectomy. A new surgical technique for primary malignant vertebral tumors. *Spine* 22-3: 324-33, 1997.

28. Tsubota, K., T. Adachi, and Y. Tomita. “Simulation study on model parameters of trabecular surface remodelling model”. In: *Computer Methods in Biomechanics & Biomedical Engineering - 3*, edited by J. Middleton, M. L. Jones, N. G. Shrive, and G. N. Pande. Gordon and Breach Science Publishers, 2001, pp. 129-134.

29. Vaccaro, A. R., and S. R. Garfin. Internal fixation (pedicle screw fixation) for fusions of the lumber spine. *Spine* 20-24S: 157S-165S, 1995.

30. Zankl, M., and A. Wittmann. The adult male voxel model "Golem" segmented from whole-body CT patient data. *Radiat. Environ. Biophys.* 40-2: 153-162, 2001.

31. Zioupos, P., C. W. Smith, and Y. H. An. "Factors affecting mechanical properties of bone". In: *Mechanical testing of bone and the bone-implant interface*, edited by Y. H. An, and R. A. Draughn. CRC Press, 1999, pp. 41-85.

Legend of Figures

FIGURE 1. Voxel-based finite element model of half of the vertebral body with a fixation screw (model S), in which symmetry with respect to the center sagittal plane was assumed. The model consisted of cortical bone, cancellous bone, and screw. The size of the voxel element was 250 μm. (a) Three-dimensional image and loading condition. Compressive load F_1 of body weight was applied to the vertebral body, and the load F_2 transferred from a fixation device was applied to the end of the screw. (b) $X_2 - X_3$ and $X_1 - X_3$ cross sections. The initial trabecular structure was oriented along axial direction, which was taken from the remodeling simulation for a normal vertebral body shown in Appendix A.

FIGURE 2. Voxel-based finite element model of cancellous bone adjacent to the bone-screw interface (model I). The model consisted of cancellous bone and screw, in which the shape of the screw threads was expressed in detail. The size of the voxel element was 70 μm. (a) Three-dimensional image. The initial trabecular structure was assumed to

be isotropic and was created by filling ring-shaped trabeculae. The white box shows the region of interest in the remodeling simulation. (b) Two cases of simple load, compression (Ic) and shear (Is), applied to the screw.

FIGURE 3. Trabecular structural changes in vertebral body with fixation screw (model S) obtained by remodeling simulation. The trabecular structural changes in regions A (above the screw) and B (below the screw) were affected by the implanted screw more than those in region F (in front of the screw). (a) Three-dimensional image and $X_2 - X_3$ and $X_1 - X_3$ cross sections. The effect of the screw was the greatest in region B where the trabecular orientation changed from the axial direction, as indicated by open and closed arrows in $X_2 - X_3$ cross section. (b) Fabric ellipsoids of trabecular structure in regions F, A, and B. Degree of structural anisotropy H_1/H_3 in region B was the smallest of the three regions and the principal direction $\square_3$ was the largest, which indicated distributed trabecular structure.

FIGURE 4. Trabecular structural changes adjacent to the bone-screw interface under compressive load (case Ic). (a) Three-dimensional image and $X_1 - X_3$ and $X_2 - X_3$ cross sections. The trabeculae were oriented along the direction of compressive load in $X_2 - X_3$ cross section, and radially aligned in $X_1 - X_3$ cross section, as indicated by

arrows. (b) Fabric ellipsoids of trabecular structure in regions C (below the screw), S_1 (on the negative side on the X_1 axis), and S_2 (on the positive side). The degree of structural anisotropy H_1/H_3 was similar in each region and the principal direction $\square_1$ was different.

FIGURE 5. Trabecular structural changes adjacent to the bone-screw interface under shear load (case Is). (a) Three-dimensional image and $X_1 \square X_3$ and $X_2 \square X_3$ cross sections. The trabeculae were oriented along 45 degrees in $X_2 \square X_3$ cross section, and distributed in $X_1 \square X_3$ cross section. (b) Fabric ellipsoids of trabecular structure in regions C, S_1, and S_2. The degree of structural anisotropy was smaller than that in the case of compressive load (Ic), indicating a more distributed structure.

FIGURE 6. Change in contact area S/S_0 between the screw threads and the trabeculae for bone-screw interface (model I). The rate of areal change depended on the site of the screw threads. (a) Compressive load (Ic). The contact area S/S_0 increased after the initial decrease at the top of the screw threads (Tt), and decreased on both sides (Ts_1 and Ts_2) and at the root (Tr). (b) Shear load (Is). The entire contact area S/S_0 decreased. The rate of decrease was higher at Ts_1 and Tr than at Tt and Ts_2

FIGURE 7. Voxel-based finite element model of half of a normal vertebral body (model N),

in which symmetry with respect to the center sagittal plane was assumed. The model consisted of cortical bone and cancellous bone. The size of the voxel element was 250 μm. (a) Three-dimensional image and compressive loading condition due to body weight (left), fabric ellipsoid of trabecular structure (right upper), and $X_2 - X_3$ cross section (right lower). Fabric ellipsoid and $X_2 - X_3$ cross section show the initial isotropic trabecular structure. (b) The shape of the cortical and cancellous bone. Three-dimensional cortical shape was constructed by rotating a midsaggital section.

FIGURE 8. Trabecular structural changes in a normal vertebral body (model N) obtained by remodeling simulation. The initial isotropic trabecular structure became anisotropic to adapt the compressive load of body weight, as shown in $X_2 - X_3$ cross section. The first principal direction θ_3 of the fabric ellipsoid was approximately equal to zero, and the degree of structural anisotropy H_1/H_3 increased to 1.47 from 1.04 at the initial stage. These structural parameters indicated that the trabecular orientation changed to the direction of axial load due to remodeling.

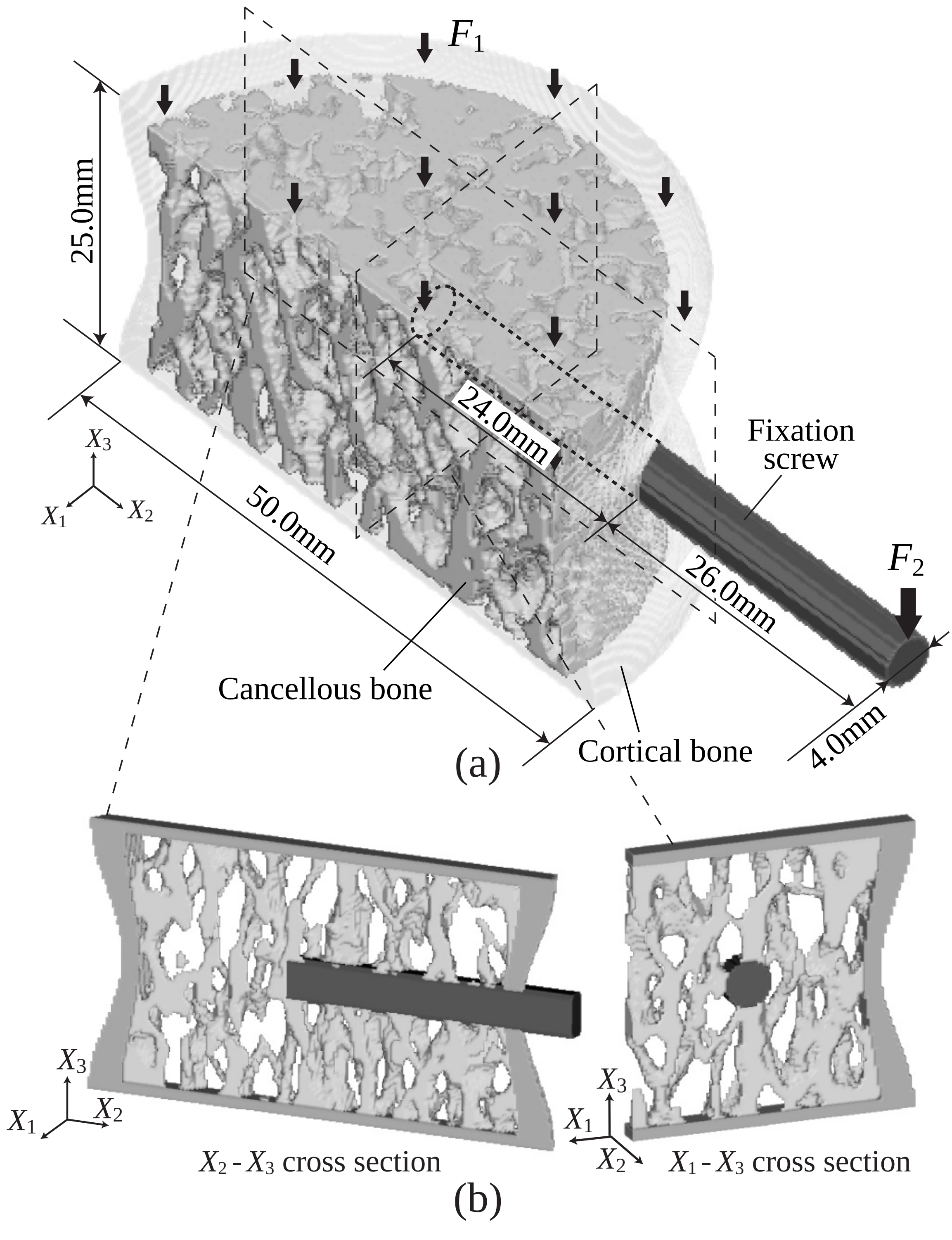

F_1
25.0mm
24.0mm
Fixation screw
X_3
X_1
X_2
50.0mm
26.0mm
F_2
Cancellous bone
4.0mm
(a)
Cortical bone
X_3
X_1
X_2
X_2 - X_3 cross section
X_3
X_1
X_2
X_1 - X_3 cross section
(b)

FIGURE 1.

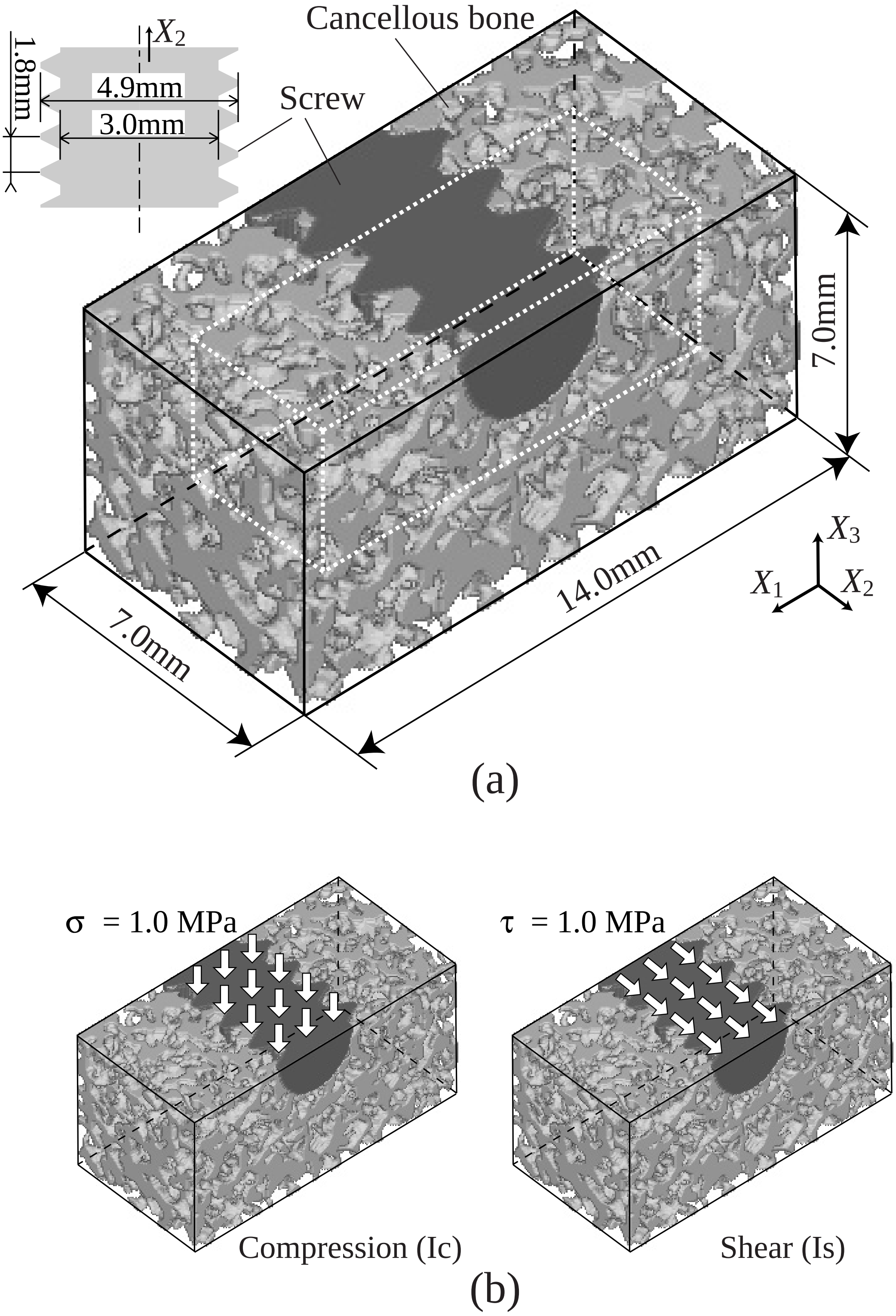

Cancellous bone
Screw
X2
1.8mm
4.9mm
3.0mm
7.0mm
14.0mm
7.0mm
X3
X1
X2
(a)
σ = 1.0 MPa
τ = 1.0 MPa
Compression (Ic)
Shear (Is)
(b)

FIGURE 2.

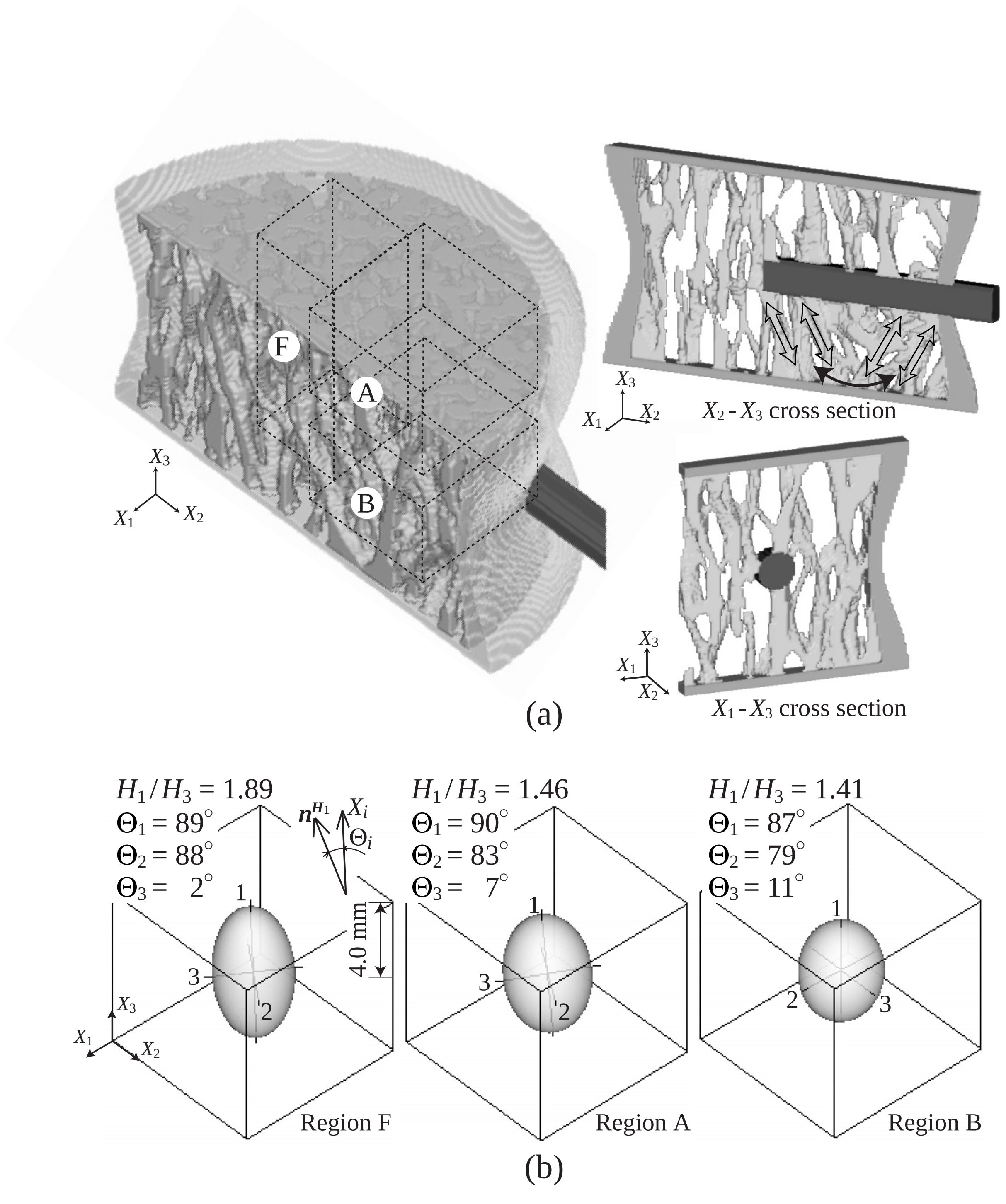
F
A
B
X_3
X_1
X_2
X_2 - X_3 cross section
X_1 - X_3 cross section
(a)
$H_1/H_3 = 1.89$
$\Theta_1 = 89^\circ$
$\Theta_2 = 88^\circ$
$\Theta_3 = 2^\circ$
$\boldsymbol{n}^{H_1}$
X_i
Θ_i
4.0 mm
Region F
$H_1/H_3 = 1.46$
$\Theta_1 = 90^\circ$
$\Theta_2 = 83^\circ$
$\Theta_3 = 7^\circ$
Region A
$H_1/H_3 = 1.41$
$\Theta_1 = 87^\circ$
$\Theta_2 = 79^\circ$
$\Theta_3 = 11^\circ$
Region B
(b)

FIGURE 3.

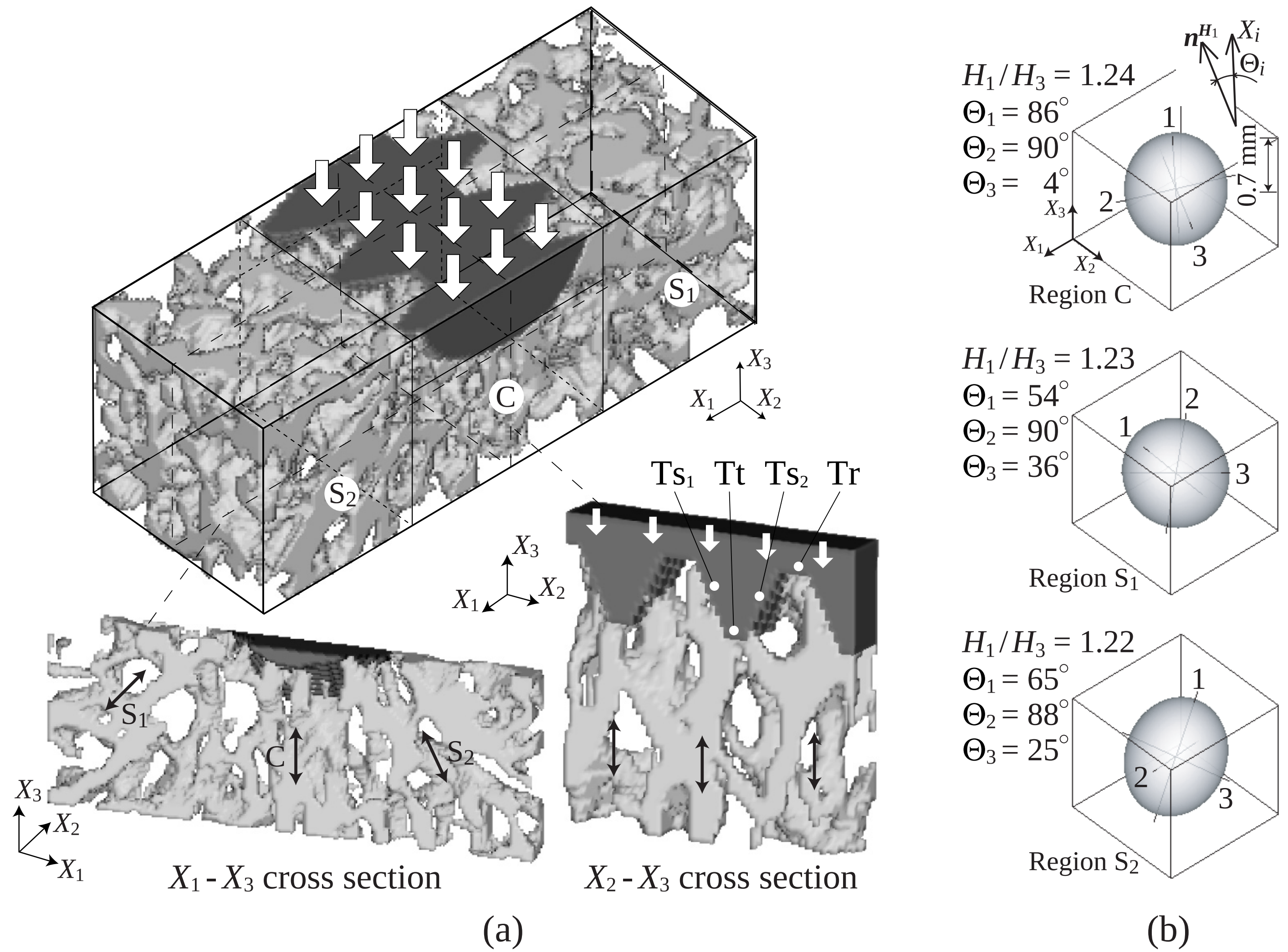

S1
C
S2
X3
X1
X2
Ts1 Tt Ts2 Tr
S1
C
S2
X1 - X3 cross section
X2 - X3 cross section
(a)
H1 / H3 = 1.24
Θ1 = 86°
Θ2 = 90°
Θ3 = 4°
0.7 mm
Region C
H1 / H3 = 1.23
Θ1 = 54°
Θ2 = 90°
Θ3 = 36°
Region S1
H1 / H3 = 1.22
Θ1 = 65°
Θ2 = 88°
Θ3 = 25°
Region S2
(b)

FIGURE 4.

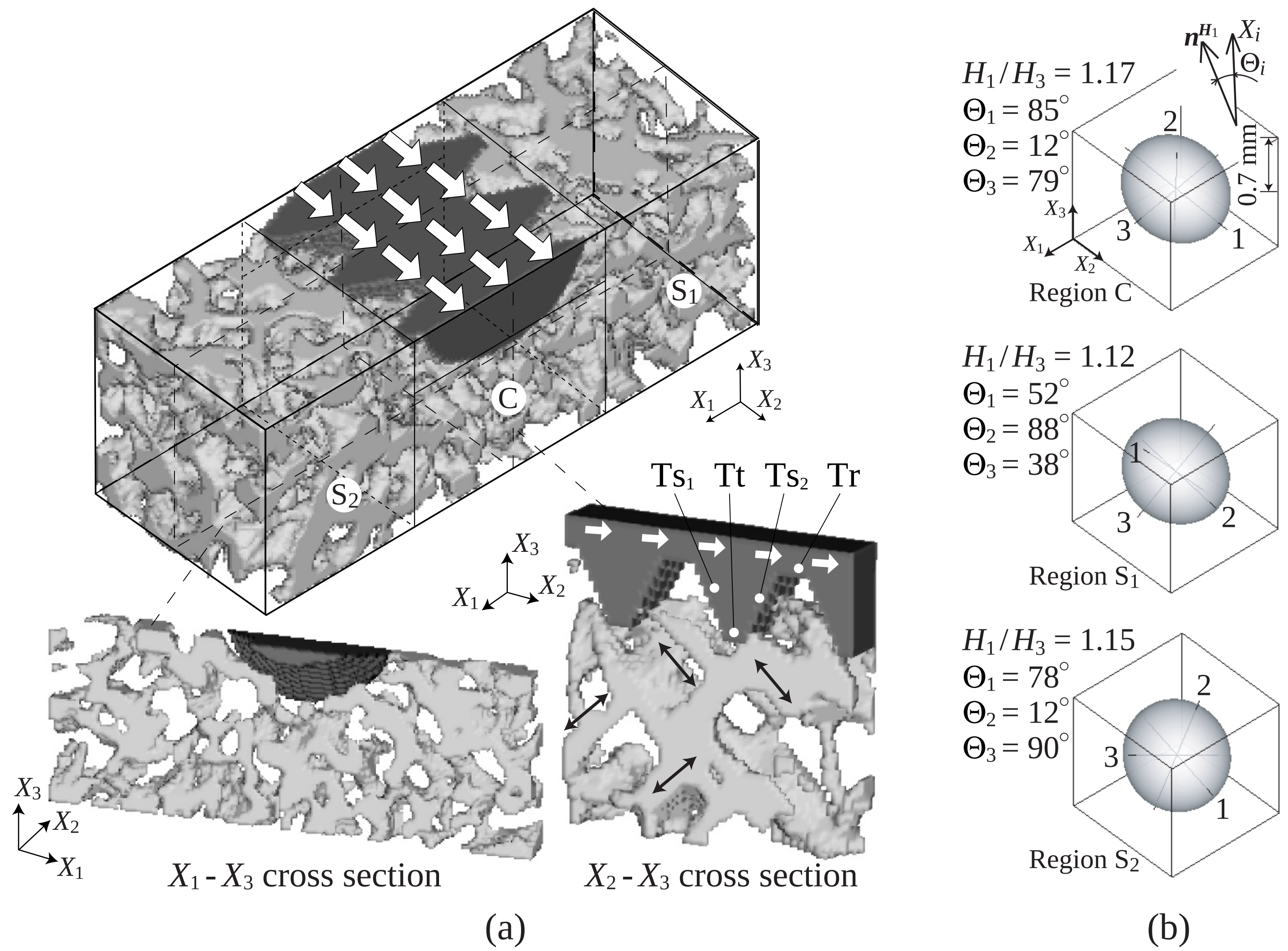
S1
C
S2
X3
X1
X2
Ts1
Tt
Ts2
Tr
X1 - X3 cross section
X2 - X3 cross section
(a)
H1 / H3 = 1.17
Θ1 = 85°
Θ2 = 12°
Θ3 = 79°
0.7 mm
Θi
Xi
2
3
1
Region C
H1 / H3 = 1.12
Θ1 = 52°
Θ2 = 88°
Θ3 = 38°
Region S1
H1 / H3 = 1.15
Θ1 = 78°
Θ2 = 12°
Θ3 = 90°
Region S2
(b)

FIGURE 5.

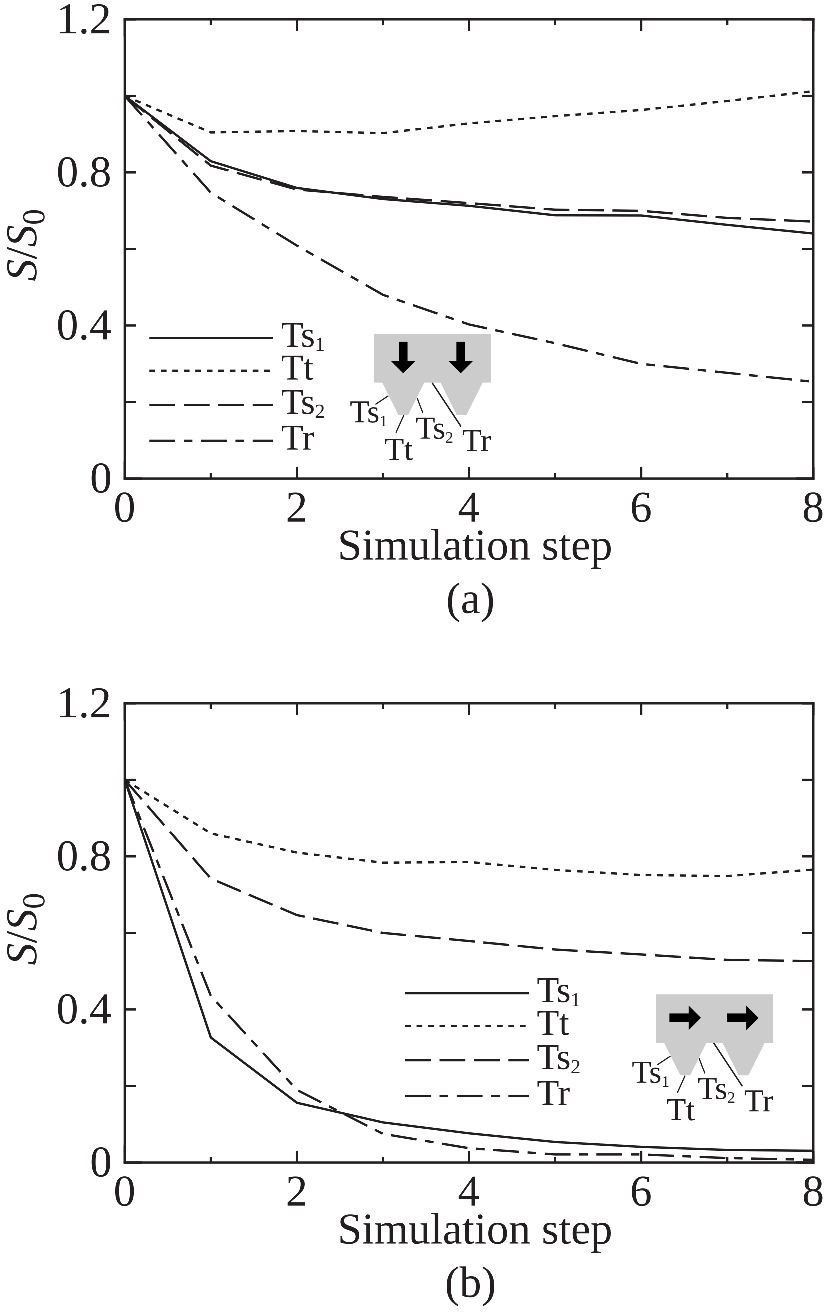

FIGURE 6.

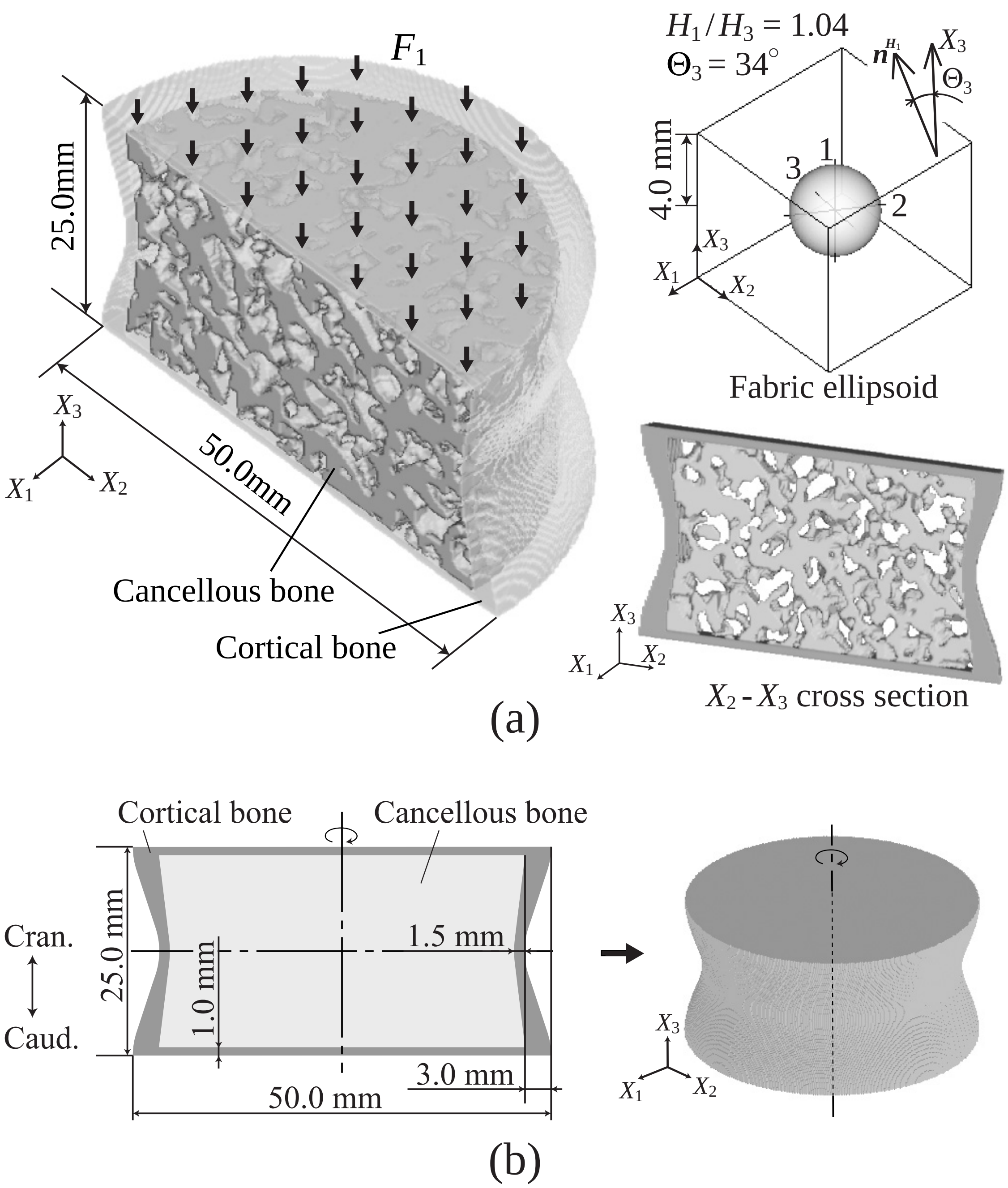

F_1
25.0mm
50.0mm
X_3
X_1
X_2
Cancellous bone
Cortical bone
$H_1/H_3 = 1.04$
$\Theta_3 = 34°$
n^{H_1}
Θ_3
4.0 mm
1
2
3
Fabric ellipsoid
X_2 - X_3 cross section
(a)
Cortical bone
Cancellous bone
Cran.
Caud.
25.0 mm
1.0 mm
1.5 mm
3.0 mm
50.0 mm
(b)

FIGURE 7.

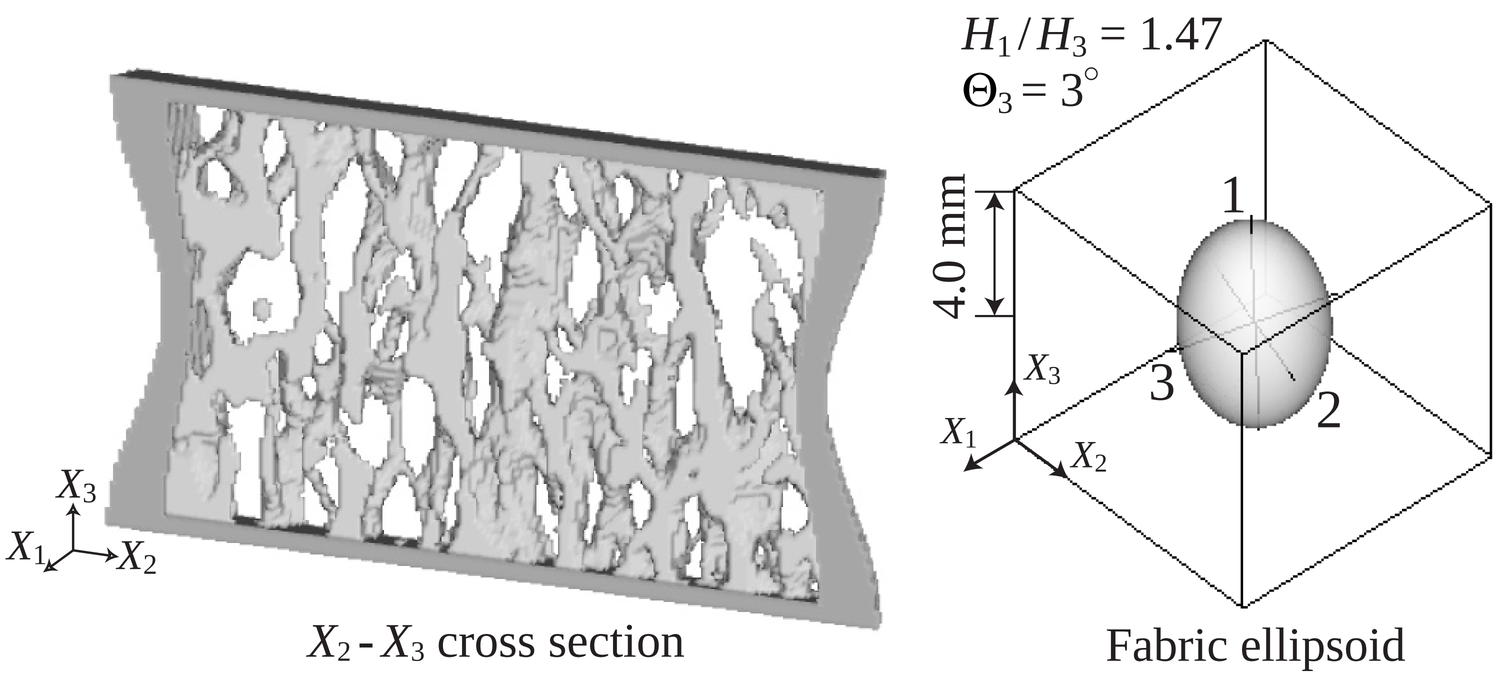
X_3
X_1
X_2
X_2 - X_3 cross section
$H_1 / H_3 = 1.47$
$\Theta_3 = 3^\circ$
4.0 mm
1
2
3
X_3
X_1
X_2
Fabric ellipsoid

FIGURE 8.